Natural convection flow of Sodium Alginate based Casson nanofluid about a solid sphere in the presence of a magnetic field with constant surface heat flux

Natural convection flow of Sodium Alginate based Casson nanofluid about a solid sphere in the presence of a magnetic field with constant surface heat flux

Firas A Alwawi[1,2,*], Hamzeh T Alkasasbeh[3], Ahmad M Rashad[4] and Ruwaidiah Idris[1]

[1]School of Informatics and Applied Mathematics, Universiti Malaysia Terengganu, 21030 Kuala Nerus, Terengganu, Malaysia
[2]Department of Mathematics, College of Sciences and Humanities in Al-Kharj, Prince Sattam bin Abdulaziz University, Al-Kharj 11942, Saudi Arabia
[3]Department of Mathematics, Faculty of Science, Ajloun National University, P.O.Box 43, Ajloun 26810, Jordan
[4]Department of Mathematics, Aswan University, Faculty of Science, Aswan, 81528, Egypt

[*]E-mail: f.alwawi@psau.edu.sa

Abstract. In this paper, we examined a free convection flow of Sodium Alginate (SA) as a host Casson fluid with three different types of nanoparticles specifically, Silicon Dioxide (SiO_2)**,** Copper oxide (CuO), and Copper (Cu) on a solid sphere in the presence of magnetic field along with prescribed surface heat flux. The Keller-box method was carried out for solving the transformed governing partial differential equations. Numerical results for the local skin friction coefficient are obtained and compared with literature. Also, the influences of Casson parameter, magnetic parameter, nanoparticles volume fraction, on local skin friction coefficient, local Nusselt number, temperature, and velocity are analyzed graphically. Our study revealed that the local Nusselt number, local skin friction coefficient and velocity profiles of SiO_2 - SA based Casson nanofluid are higher than the other nanoparticles - SA based Casson nanofluid, as well as it has the lowest temperature profiles.

1. Introduction

Casson fluid is a subclass of non-Newtonian fluid which behaves like an elastic solid where no flow occurs with small shear stress. It was first introduced by Casson [1] in 1959 to predict the flow behavior for pigment-oil suspensions of the printing ink. Later on, numerous articles have been done on the same field. Mustafa et al. [2, 3] studied the flow of a Casson fluid over a semi-infinite flat plate with a parallel free stream and in the region of stagnation point towards a stretching sheet. Nadeema et al. [4] investigated the boundary layer three-dimensional flow of Casson fluid over a stretching sheet. Several studies on Casson fluids can also be found in these references [5-11]. Sodium alginate is one of the most fluids that has ever been used in many industries for over a century since it was discovered by the British

pharmacist Stanford [12, 13] in 1881, where it is used in food manufacturing, pharmaceuticals, textiles and cosmetics. Sodium alginate has received much attention by researchers, Hatami and Ganji [14, 15] investigated the heat transfer of Sodium alginate nanofluid flow in the porous area between two coaxial cylinders and between two vertical flat plates. For more reading see the following references [16-18].

Recently, a new class of fluids called nanofluids was introduced to improve the thermal properties of conventional base fluids by adding nanoparticles to ordinary base fluids. The concept of nanofluids was reported by Chol and Estman [19] where he introduced the idea of nanoparticles suspended in a host fluid. Eastman et al. [20] found that the addition of copper (10 nm) particles in ethylene glycol increases the thermal conductivity up to 40%. Chon et al. [21] examined the effect of temperature and nanoparticle size on thermal conductivity of nanofluid. Here are some significant researches on nanofluids [22-30].

MHD natural convection on a sphere has received considerable attention over recent decades and the significance of this issue due to the wide range applications in numerous modern industrials, where a number of papers have been published in this field, Huang and Chen [31] investigated the impact of Prandtl number and surface mass transfer on a steady, laminar of natural convective flow about a solid sphere with constant surface heat flux. Kumari et al. [32] examined MHD flow of an electrically conducting fluid in the stagnation region of a sphere. Nazar et al. [33] studied numerically the natural convection flow past a sphere with prescribed surface heat flux in a micropolar fluid. Chamkha and Al-Mudhaf [34] analyzed the influence of the magnetic field and thermal radiation on free convection from a permeable sphere. Alkasasbeh [35] studied the natural convection flow of Casson micropolar fluid over a solid sphere in the presence of a magnetic field. Also, [36-39] all of them investigated the impact of heat generation and magnetic field on free convection over a sphere.

In this paper, we examined MHD free convection flow of Sodium alginate nanofluid on a solid sphere with constant surface heat flux by using the Keller box method which is neither published nor considered in the scientific literature.

2. Mathematical modeling

A steady state two-dimensional laminar MHD free convective flow of Copper (Cu), Copper oxide (CuO), and Silicon Dioxide (SiO_2) **-** Sodium Alginate based Casson nanofluid from a solid sphere of the radius a and prescribed surface heat flux q_w are considered. Figure 1 presents the Physical model and coordinate system, where g is the gravity vector, T_∞ is the ambient temperature of the nanofluid, β_0^2 is the magnetic field strength , x^* - coordinate is measured along the surface of the solid sphere at the lower stagnation point $(x^* \approx 0)$, y^* – coordinate is measured the distance normal to the surface of the sphere and $r^*(x^*)$ is the radial distance from the symmetrical axis to the surface of the solid sphere.

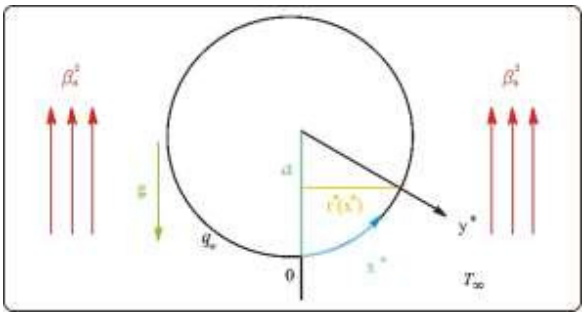

Figure 1. Physical model and coordinate system.

The Casson fluid flow is reported by Ahmed and Khan [17] :

$$\tau_{ij} = \begin{cases} 2\left(\mu_B + p_y\sqrt{2\pi}\right)e_{ij} & \pi > \pi_c, \\ 2\left(\mu_B + p_y\sqrt{2\pi_C}\right)e_{ij} & \pi < \pi_c, \end{cases} \tag{1}$$

where $\pi = e_{ij}e_{ij}$, e_{ij} is the (i, j)-th component of the deformation rate, μ_β is the plastic dynamic viscosity of the non-Newtonian fluid, p_y is the yield stress of the fluid and π_c is a critical value of this product.

The continuity, momentum and energy equations of the steady incompressible Casson nanofluid boundary layer flow can be expressed as:

$$\frac{\partial}{\partial x^*}\left(r^* u^*\right) + \frac{\partial}{\partial y^*}\left(r^* v^*\right) = 0, \tag{2}$$

$$u^* \frac{\partial u^*}{\partial x^*} + v^* \frac{\partial u^*}{\partial y^*} = \frac{\mu_{nf}}{\rho_{nf}}\left(1 + \frac{1}{\beta}\right)\frac{\partial^2 u^*}{\partial y^{*2}} + \left(\frac{\chi\rho_s\beta_s + (1-\chi)\rho_f\beta_f}{\rho_{nf}}\right)g\left(T - T_\infty\right)\sin\left(\frac{x^*}{a}\right) - \frac{\sigma_{nf}\beta_0^2}{\rho_{nf}}u^*, \tag{3}$$

$$u^* \frac{\partial T}{\partial x^*} + v^* \frac{\partial T}{\partial y^*} = \alpha_{nf}\frac{\partial^2 T}{\partial y^{*2}} \tag{4}$$

subject to the boundary conditions defined by Molla et al. [37]:

$$\begin{gathered} u^* = v^* = 0, \ \frac{\partial T}{\partial y^*} = \frac{-q_w}{k}, \ \text{as} \ y^* = 0, \\ u^* \to 0, T \to T_\infty, \ \text{as} \ y^* \to \infty, \end{gathered} \tag{5}$$

where $\left(u^*, v^*\right)$ are the velocity components along the $\left(x^*, y^*\right)$ directions, β is the Casson parameter, T is the temperature , χ, β_s, and ρ_s are volume fraction, thermal expansion coefficient, and the density of nanoparticles, respectively. $\sigma_f, \rho_f, \mu_f, \nu_f$ and β_f are electrical conductivity, density, viscosity, kinematic viscosity and the thermal expansion coefficient of the host fluid, respectively. $\sigma_{nf}, \alpha_{nf}, \rho_{nf}, (\rho c_p)_{nf}, \mu_{nf}$ and k_{nf} are electrical conductivity, thermal diffusivity, density, viscosity, heat capacity and the thermal conductivity of the nanofluid, respectively which defined by Zangooee et. al [40] :

$$\begin{gathered} \frac{\sigma_{nf}}{\sigma_f} = 1 + \frac{3(\sigma - 1)\chi}{(\sigma + 2) - (\sigma - 1)\chi}, \ \sigma = \frac{\sigma_s}{\sigma_f}, \ \frac{k_{nf}}{k_f} = \frac{\left(k_s + 2k_f\right) - 2\chi\left(k_f - k_s\right)}{\left(k_s + 2k_f\right) + \chi\left(k_f - k_s\right)}, \ \mu_{nf} = \frac{\mu_f}{(1-\chi)^{2.5}}, \\ \left(\rho c_p\right)_{nf} = (1-\chi)\left(\rho c_p\right)_f + \chi\left(\rho c_p\right)_s, \ \rho_{nf} = (1-\chi)\rho_f + \chi\rho_s, \ \alpha_{nf} = \frac{k_{nf}}{\left(\rho c_p\right)_{nf}}, \end{gathered} \tag{6}$$

here k_s is thermal conductivity of nanoparticles and k_f is thermal conductivity of host fluid.

Now, we will introduce the following non-dimensional variables [37]:

$$x = \frac{x^*}{a}, \ y = Gr^{1/5}\left(\frac{y^*}{a}\right), \ r(x) = \frac{r^*(x^*)}{a}, \ u = \left(\frac{a}{\nu_f}\right)Gr^{-2/5}u^*,$$

$$\theta = Gr^{1/5}\left(\frac{T-T_\infty}{aq_w/k}\right),\ v = \left(\frac{a}{\nu_f}\right)Gr^{-1/5}v^* \tag{7}$$

where $Gr = g\beta_f(aq_w/k)\frac{a^3}{\nu_f^2}$ is the Grashof number and $r^*(x^*)$ is the radial distance from the symmetrical axis to the surface of the solid sphere and is given by :

$$r^*(x^*) = a\sin\left(\frac{x^*}{a}\right) \tag{8}$$

Substitute equations (7) and (8) into equations (2) - (5) to obtain the following non-dimensional equations:

$$\frac{\partial}{\partial x}(r\,u) + \frac{\partial}{\partial y}(r\,v) = 0, \tag{9}$$

$$\left(u\frac{\partial u}{\partial x} + v\frac{\partial u}{\partial y}\right) = \frac{\rho_f}{(1-\chi)^{2.5}\rho_{nf}}\left(1+\frac{1}{\beta}\right)\frac{\partial^2 u}{\partial y^2} + \left(\frac{\chi\rho_s(\beta_s/\beta_f)+(1-\chi)\rho_f}{\rho_{nf}}\right)\theta\sin x - \frac{\sigma_{nf}\rho_f}{\sigma_f\rho_{nf}}Mu \tag{10}$$

$$u\frac{\partial\theta}{\partial x} + v\frac{\partial\theta}{\partial y} = \frac{1}{\Pr}\frac{k_{nf}/k_f}{\left((1-\chi)(\rho C_p)_f + \chi(\rho C_p)_s/(\rho C_p)_f\right)}\frac{\partial^2\theta}{\partial y^2}, \tag{11}$$

subject to the boundary conditions:

$$\begin{aligned} &u = v = 0,\ \frac{\partial\theta}{\partial y} = -1 \text{ as } y = 0, \\ &u \to 0,\ \theta \to 0 \text{ as } y \to \infty \end{aligned} \tag{12}$$

here $M = \frac{\sigma_f\beta_0^2 a^2 Gr^{-2/5}}{\nu_f\rho_f}$ is the magnetic parameter and $\Pr = \frac{\alpha_f}{\nu_f}$, is the Prandtl number.

To solve equations (9)-(11) along with the boundary conditions (12), defined the following variables:

$$\psi = xr(x)F(x,y),\ \theta = \theta(x,y), \tag{13}$$

where ψ is the stream function expressed as :

$$u = \frac{1}{r}\frac{\partial\psi}{\partial y} \text{ and } v = -\frac{1}{r}\frac{\partial\psi}{\partial x} \tag{14}$$

which satisfies equation (9). Thus, equations (10) and (11) can be expressed as follows:

$$\begin{aligned} &\frac{\rho_f}{(1-\chi)^{2.5}\rho_{nf}}\left(1+\frac{1}{\beta}\right)\frac{\partial^3 F}{\partial y^3} + (1+x\cot x)F\frac{\partial^2 F}{\partial y^2} - \left(\frac{\partial F}{\partial y}\right)^2 - \frac{\sigma_{nf}\rho_f}{\sigma_f\rho_{nf}}M\frac{\partial F}{\partial y} \\ &\quad + \left(\frac{\chi\rho_s(\beta_s/\beta_f)+(1-\chi)\rho_f}{\rho_{nf}}\right)\theta\frac{\sin x}{x} = x\left(\frac{\partial F}{\partial y}\frac{\partial^2 F}{\partial x\partial y} - \frac{\partial F}{\partial x}\frac{\partial^2 F}{\partial y^2}\right) \end{aligned} \tag{15}$$

$$\begin{aligned} &\frac{1}{\Pr}\frac{k_{nf}/k_f}{\left((1-\chi)(\rho C_p)_f + \chi(\rho C_p)_s/(\rho C_p)_f\right)}\frac{\partial^2\theta}{\partial y^2} + (1+x\cot x)F\frac{\partial\theta}{\partial y} \\ &\quad = x\left(\frac{\partial F}{\partial y}\frac{\partial\theta}{\partial x} - \frac{\partial F}{\partial x}\frac{\partial\theta}{\partial y}\right) \end{aligned} \tag{16}$$

subject to

$$\frac{\partial F}{\partial y}=0,\ F=0,\ \ \frac{\partial \theta}{\partial y}=-1 \text{ as } y=0,$$
$$\frac{\partial F}{\partial y}\to 0,\ \ \theta\to 0, \text{ as } y\to\infty \tag{17}$$

At the lower stagnation point of the sphere $(x\approx 0)$, equations (15) and (16) reduce to the following ordinary differential equations:

$$\frac{\rho_f}{(1-\chi)^{2.5}\rho_{nf}}\left(1+\frac{1}{\beta}\right)F'''+2FF''-\left(\frac{\partial F}{\partial y}\right)^2-\frac{\sigma_{nf}\rho_f}{\sigma_f\rho_{nf}}M\ F'+\left(\frac{\chi\rho_s\left(\beta_s/\beta_f\right)+(1-\chi)\rho_f}{\rho_{nf}}\right)\theta=0 \tag{18}$$

$$\frac{1}{\Pr}\frac{k_{nf}/k_f}{\left((1-\chi)(\rho C_p)_f+\chi(\rho C_p)_s/(\rho C_p)_f\right)}\theta''+2F\theta'=0 \tag{19}$$

and the boundary conditions (17) become:

$$F'(0,y)=0,\ F(0,y)=0,\ \theta'(0)=-1 \quad \text{as} \quad y=0,$$
$$F'\to 0,\ \theta\to 0, \text{ as} \quad y\to\infty \tag{20}$$

In this artical we interest in two physical quantities specifically, the local skin friction coefficient C_f and the local Nusselt number Nu, which are given by Molla et al. [37]:

$$C_f=\frac{a^2\tau_w}{\rho U^2},\ \ Nu=\frac{aq_w}{k_f(T-T_\infty)} \tag{21}$$

where

$$\tau_w=\mu_{nf}\left(\frac{\partial u^*}{\partial y^*}\right)_{y^*=0},\quad q_w=-k_{nf}\left(\frac{\partial T}{\partial y^*}\right)_{y^*=0}. \tag{22}$$

Use the non-dimensional variables (7) and boundary conditions (17), the local skin friction coefficient C_f and Nusselt number Nu are:

$$C_f^*=\frac{1}{(1-\chi)^{2.5}}\left(1+\frac{1}{\beta}\right)x\frac{\partial^2 F}{\partial y^2}(x,0),\ \ Nu^*=\frac{k_{nf}}{k_f}\left(\frac{1}{\theta(x,0)}\right) \tag{23}$$

here $C_f^*=Gr^{1/5}C_f$, and $Nu^*=Gr^{-1/5}Nu$.

3. Numerical method

The nonlinear differential equations (15) and (16) along with boundary conditions (17) have been computed numerically by utilizing the Keller box technique. It is unconditionally stable, has second-order accuracy and the results are achieved in a reasonable time, this method can be summarized as the following: First, we reduce the transformed equations (15) and (16) to a first-order system. Next, we write the difference equations using central differences. After that, we linearize the resulting algebraic equations by Newton's method and write them in matrix-vector form. Lastly, we solve the linear system by the block tridiagonal elimination technique. For more details of this technique see the following refs. [41-43]

4. Numerical results and discussion

Table 1 presents the thermo-physical properties of nanoparticles and Sodium Alginate, whereas table 2 shows a numerical comparison of local skin friction coefficient C_f with Newtonian fluid.

Table 1. Thermo-physical properties of SiO_2, CuO, Cu and SA as a host Casson fluid [44-48].

Thermo-Physical property	SA	CuO	Cu	SiO_2
$\rho\left(kg/m^3\right)$	989	6500	8933	2220
$C_p\left(J/kgK\right)$	4175	540	385	745
$K\left(w/mK\right)$	0.6376	18	401	1.38
$\beta\times10^{-5}\left(K^{-1}\right)$	99	0. 85	1.67	0.055
$\sigma\left(s/m\right)$	2.6×10^{-4}	59.5×10^{6}	59.6×10^{6}	10^{-21}
Pr	6.45	-	-	-

Table 2. Comparison of local skin friction coefficient C_f with Newtonian fluid $\left(\beta\to\infty, M=0,\ \chi=0\right)$ at $\mathrm{Pr}=0.7$.

x	Huang and Chen [31]	Nazar et al.[33]	Present
0^o	0.0000	0.0000	0.000000
10^o	0.2138	0.2138	0.212301
20^o	0.4247	0.4246	0.415758
30^o	0.6299	0.6297	0.625222
40^o	0.8265	0.8260	0.820074
50^o	1.0118	1.0110	1.00337
60^o	1.1828	1.1815	1.16766
70^o	1.3376	1.3356	1.31984
80^o	1.4708	1.4678	1.45194
90^o	1.5818	1.5780	1.56094
100^o	-	1.6614	1.64355
110^o	-	1.7140	1.69601
120^o	-	1.7314	1.71361

Figure 2(a and b) depicts the effect of χ on C_f^* and Nu^* respectively, it is found that by increasing χ, both C_f^* and Nu^* increase , this dependence of Nu^* and C_f^* on χ can be additionally clarified by looking at equation (23). figure 3(a and b) illustrates the impact of β on C_f^* and Nu^* respectively, we found that an increase in Casson parameter causes a decrement in the local skin friction coefficient and a rise in the local Nusselt number, but when x increase, the local skin friction coefficient is increasing and

the local Nusselt number is decreasing. figure 4(a and b) shows the influnce of M on C_f^* and Nu^* respectively, it's clear from this figure that an increase in the intensity of the magnetic field led to reducing the skin friction coefficient, this is because the application of a magnetic field leads to curb fluid

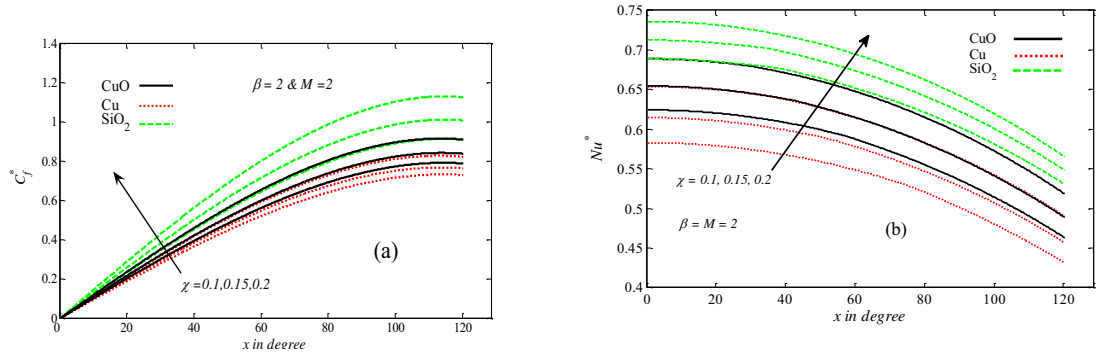

Figure 2. Influence of χ on C_f^* and Nu^*.

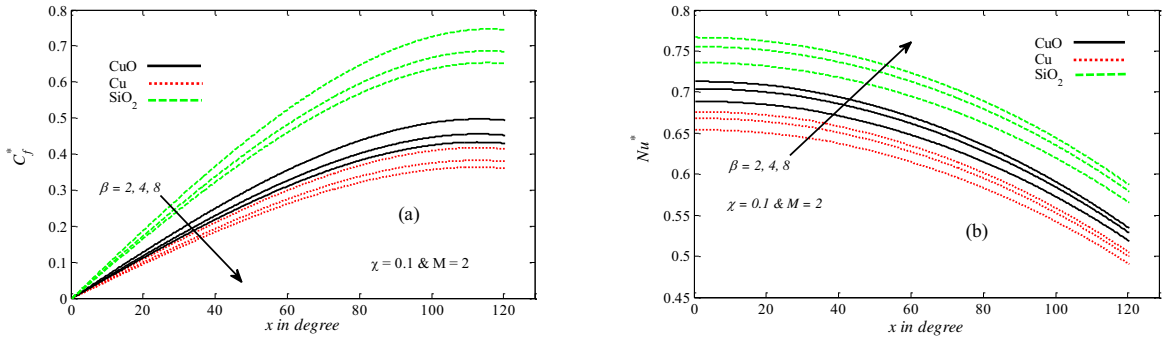

Figure 3. Influence of β on C_f^* and Nu^*.

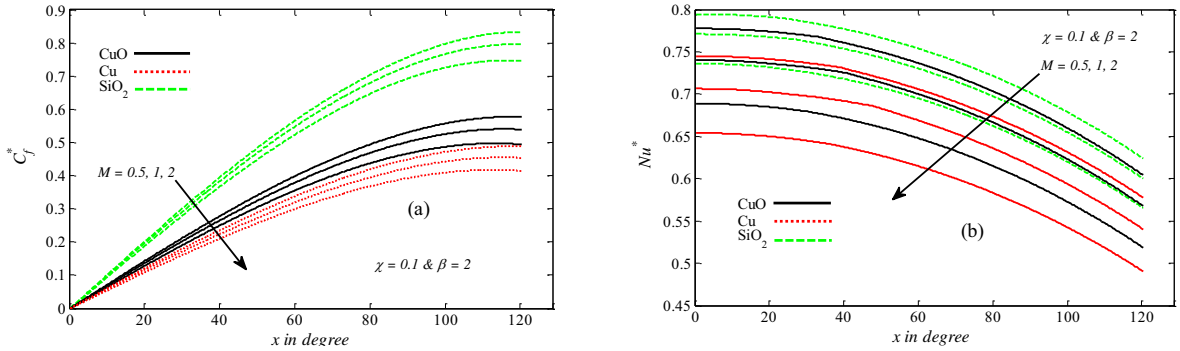

Figure 4. Influence of M on C_f^* and Nu^*.

flow hence reducing the surface friction force, also an increase in M led to reducing Nu^*. Moreover, figures 2-4 reveal that the rate heat transfer of Cu-SA is the lowest as compared with other nanoparticles SA, and SiO_2 - SA produced the highest skin friction followed by CuO –SA while Cu – SA produced

lowest skin friction. Figure 5(a and b) presents the impact of χ on velocity and temperature profiles respectively,

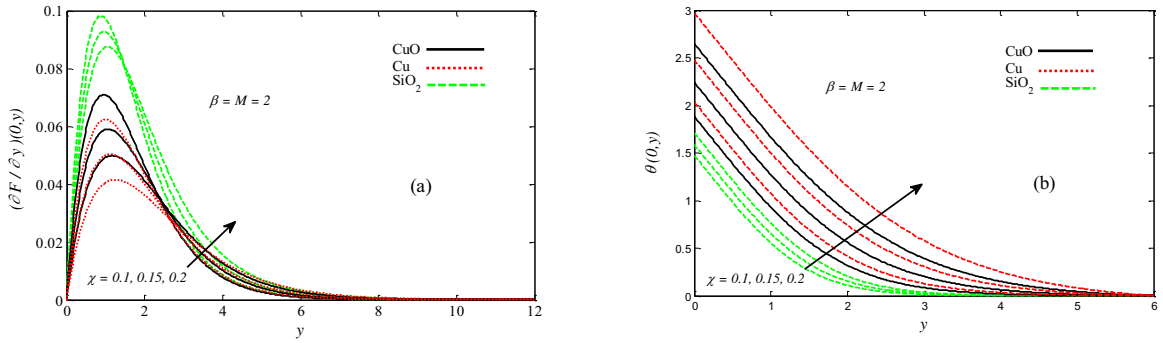

Figure 5. Impact of χ on velocity and temperature profiles.

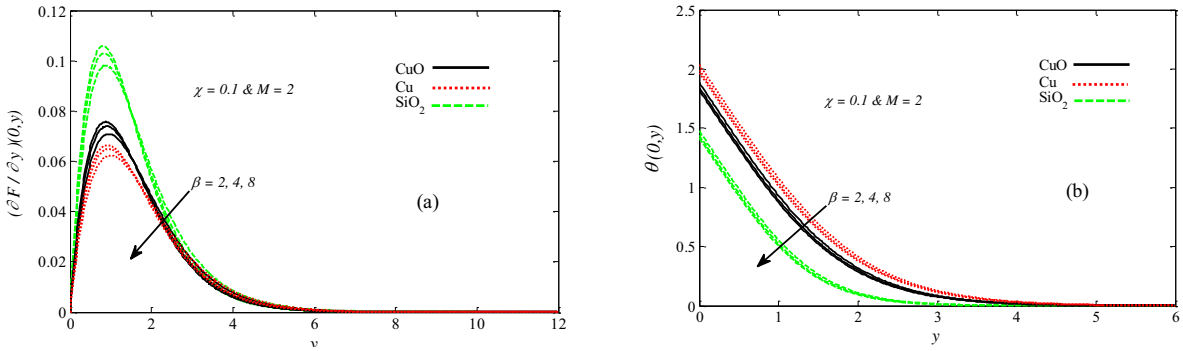

Figure 6. Impact of β on velocity and temperature profiles.

it is obvious that as χ increases, the velocity profiles increases. Also, the temperature profiles increase when χ increases and this is due to the reason that an increase in nanoparticle volume fraction leads to increases in thermal Conductivity of nanofluid which increases nanofluid's temperature. Figure 6 (a and b) displays the influnce of β on velocity and temperature respectively, it provides that an increase in β parameter contributes to the reduction of velocity temperature profiles. Figure 7(a and b) states impact of M on

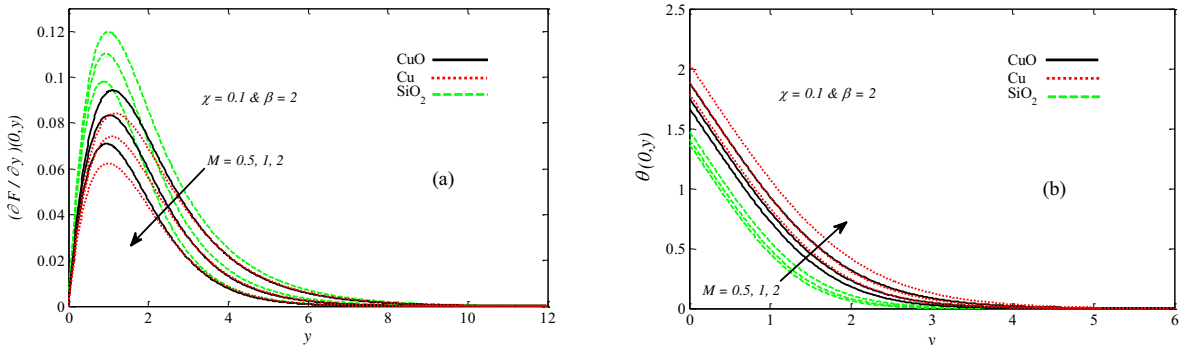

Figure 7. Impact of M on velocity and temperature profiles.

on velocity and temperature profiles, here we notice that an increase in M leads to a decrease in velocity due to increasing dragging force, while exactly opposite behavior was observed with temperature where the increase in M lead to reduce it. Further, figures 5-7 are shown that the motion of SiO_2-SA is the highest as compared with other nanoparticles - SA, and SiO_2- SA produced the lowest temperature followed by CuO –SA while Cu – SA produced the highest temperature.

5. Conclusion

MHD 2-D incompressible natural convection flow of Sodium Alginate nanofluid past a solid sphere was numerically analyzed in this article. Constant surface heat flux was also considered. Numerical solutions are obtained by the Keller box method, and graphical results are gained through MATLAB software. Results of local skin friction coefficient are compared with prior published results, and very good accuracy is accomplished with those results. According to the current study, the following can be inferred:

i. C_f^* is directly proportional to χ but it is inversely proportional to both β and M, as well as SiO_2- SA produced the highest local skin friction.
ii. Nu^* is directly proportional to both χ and β but it is inversely proportional to M, as well as SiO_2- SA has the highest local Nusselt number.
iii. An increment in χ is offset by an increment in velocity, whereas an increment in β or M is offset by a decrement in velocity
iv. An increment in χ or M is offset by an increment in temperature, whereas an increment in β is offset by a decrement in temperature.
v. The velocity of SiO_2-SA is the highest and it produced the lowest temperature.

Acknowledgment

The authors would like to acknowledge Postgraduate Management Center, University Malaysia Terengganu (UMT) for the financial support through vote numbers 62958 for this research.

References:

[1] Casson N 1959 *Rheology of disperse systems* **2** 84.
[2] Mustafa M, Hayat T, Pop I and Aziz A 2011 *Heat. Trans. Asian Res.* **40** 563.
[3] Mustafa M, Hayat T, Ioan P and Hendi A 2012 *Zeit. für Naturforschung A* **67** 70.
[4] Nadeem S, Haq R U, Akbar N S and Khan Z H 2013 *Alexandria Eng. J* **52** 577.
[5] Hayat T, Shehzad S and Alsaedi A. 2012 *Appl. Math. Mecha.* **33** 1301.
[6] Nadeem S, Haq R U and Akbar N S 2014 *IEEE. Trans. Nano-techn* **13** 109.
[7] Bhattacharyya K, Hayat T and Alsaedi A 2013 *Chin. Phys. B* **22** 024702.
[8] Qing J et al. 2016 *Entropy* **18** 123.
[9] Abolbashari M H, Freidoonimehr N, Nazari F and Rashidi M M 2015 *Advan. Powder. Techn* **26** 542.
[10] Hussanan A, Salleh M Z, Alkasasbeh H T and Khan I 2018 *Heat. Trans. Rese.* **49**.
[11] Alkasasbeh H T, Abu-Ghurra S and Alzgool H A 2019 *JP J.l Heat.Mass. Tran.* **16**:1.
[12] Stanford E 1881 *British Patent* **142**.
[13] Stanford E 1883 *Amer. J. Pharm.* **47** 617.
[14] Hatami M and Ganji D 2013 *J. Molecular. Liquids* **188** 155.
[15] Hatami M and Ganji D 2014 *Case. Stud. Thermal. Eng.* **2** 14.
[16] Akinshilo A T, Olofinkua J O and Olaye O 2017 *J. Appl. Computa. Mecha.* **3** 258.

[17] Ahmed T N and Khan I 2018 *Results. Phys.* **8** 752.
[18] Tlili I, Khan W and Khan I 2018 *Results. Phys.* **8** 213.
[19] Chol S and Estman J 1995 *ASME. Publ. Fed.* **231** 99.
[20] Eastman J A et al. 2001 *Appl. Phys. Lett.* **78** 718.
[21] Chon C H, Kihm K D, Lee S P and Choi S U 2005 *Appl. Phys. Lett.* **87** 153107.
[22] Das S K, Choi S U, Yu W and Pradeep T 2007 *Nanofluids: science and technology* (Hoboken: John Wiley and Sons).
[23] Wang X-Q and Mujumdar A S 2008 *Brazil. J. Chem. Eng.* **25** 613.
[24] Trisaksri V and Wongwises S 2007 *Renewable. Sustainable Ener. Revi.* **11** 512.
[25] Swalmeh M Z, Alkasasbeh H T, Hussanan A and Mamat M 2018 *Results. Phys.* **9** 717.
[26] Kuznetsov A and Nield D 2010 *Int. J. Therm. Sci.* **49** 243.
[27] Sheikholeslami M, Gorji-Bandpy M and Ganji D 2013 *Energy* **60** 501.
[28] Alkasasbeh H T, Swalmeh M Z, Hussanan A and Mamat M 2019 *CFD. Letters* **11** 70.
[29] Ishak N, Hussanan A, Mohamed M K A, Rosli N and Salleh M Z 2019 *AIP Conf. Proc.*
[30] Mohamed M K A, Sarif N M, Noar N A Z M, Salleh M Z and Ishak A M 2018 *Malays. J. Funda. Appl. Sci.* **14** 32.
[31] Huang M and Chen G. 1987 *J. Heat. Tran.* **109**.
[32] Kumari M, Takhar H and Nath G. 1990 *Int. J. Eng. Sci*. **28** 357.
[33] Nazar R M, Amin N, Groşan T and Pop I. 2002 *Int. Commun. Heat. Mass. Trans.* **29** 1129.
[34] Chamkha A J and Al-Mudhaf A 2004 *Numer. Heat Trans.Part A* **46** 181.
[35] Alkasasbeh H T 2018 *J. Adva. Rese. Fluid. Mecha. Thermal Sci.* **50** 55.
[36] Molla M M, Taher M, Chowdhury M M and Hossain M A 2005 *Nonlinear. Analy. Model. Control.* **10** 349.
[37] Molla M, Hossain M and Taher M 2006 *Acta. Mecha.* **186** 75.
[38] Bég O A, Zueco J, Bhargava R and Takhar H S 2009 *Int. J. Ther. Sci.* **48** 913.
[39] Haque M R, Alam M M, Ali M and Sheikh M N 2014 *European Scient. J.* **10**.
[40] Zangooee M, Hosseinzadeh K and Ganji D 2019 *Case. Studies. Ther. Eng.* **14** 100460.
[41] Cebeci T, Bradshaw P, 2012 *Physical and Computational Aspects of Convective Heat Transfer* (New York :Springer Science & Business Media) p 487.
[42] Malik M, Khan M, Salahuddin T, Khan I, 2016 *Eng. Sci. Tech. Int. J.* **19** 1985.
[43] Mohamed M 2018 *Keller-Box Method Partial Differential Equations in Boundary Layer flow of Nanofluid* (Drb-Hicom University Publisher 1, ISBN 978-967-16676-0-6).
[44] Talib S, Azmi W, Zakaria I, Mohamed W, Mamat A, Ismail H and Daud W. 2015 *Energy. Procedia* **79** 366.
[45] Tian X-Y, Li B-W and Hu Z-M 2018 *Int. J. Heat. Mass Tran.* **127** 768.
[46] Pal D and Mandal G 2015 *Powder. Techn.* **279** 61.
[47] Hakeem A A, Saranya S and Ganga B 2017 *J. Molec. Liqu.* **230** 445.
[48] Ghadikolaei S, Hosseinzadeh K and Ganji D 2018 *J. Molec. Liqu.* **272** 226.